SAND--97-0909C SAND97-0909C
CONF-970231--28

Fabrication issues of oxide-confined VCSELs

K. M. Geib, K. D. Choquette, H. Q. Hou, and B. E. Hammons

Center for Compound Semiconductor Technologies
Sandia National Laboratories
Albuquerque, NM 87185-0603

ABSTRACT

To insert high performance oxide-confined vertical-cavity surface-emitting lasers (VCSELs) into the manufacturing arena, we have examined the critical parameters that must be controlled to establish a repeatable and uniform wet thermal oxidation process for AlGaAs. These parameters include the AlAs mole fraction, the sample temperature, the carrier gas flow and the bubbler water temperature. Knowledge of these critical parameters has enabled the compilation of oxidation rate data for AlGaAs which exhibits an Arrhenius rate dependence. The compositionally dependent activation energies for $Al_xGa_{1-x}As$ layers of x=1.00, 0.98 and 0.92 are found to be 1.24, 1.75, and 1.88 eV, respectively.

Keywords: AlGaAs oxidation, wet oxidation, oxide-confined, vertical-cavity surface-emitting laser

1. INTRODUCTION

Significant advances in vertical-cavity surface-emitting laser (VCSEL) performance have been realized by employing wet thermal oxidation[1] of selected $Al_xGa_{1-x}As$ layers[2] in the device structure to form the current apertures and to provide lateral index guiding for the lasing mode[2,3]. These performance advances in monolithic oxide-confined VCSELs include extremely low threshold currents[3,4], low operating voltages[2], high wall plug efficiencies[5,6] and promising lifetimes[7]. To transfer this technology into the manufacturing arena will require a thorough understanding of the oxidation process, the apparatus and the influence of the experimental parameters on the VCSEL performance. Subtle differences in the oxidation systems and in the process parameters used by various research groups will likely cause variation in the experimental data being reported[8-11]. This paper will provide details of the control required for a manufacturable compound semiconductor oxidation process in an oxidation system we have constructed and will illustrate some of the problems and solutions we have encountered in the past 3 years of operation. We also present data on the measured oxidation rates as a function of process parameters (e.g. gas flow, bubbler temperature, etc.) and the oxidation activation energies for $Al_xGa_{1-x}As$ compositions of x=1.0, 0.98, and 0.92 along with our present understanding of the oxidation process.

2. OXIDATION SYSTEM CONFIGURATION

The wet thermal oxidation system has evolved from a simple beaker on a hot plate with crude gas flow control and a single zone tube furnace to a constant temperature bubbler bath, mass flow gas control, and a 3 zone tube furnace. The objective has been to achieve optimum control, repeatability, and uniformity of the wet oxidation of VCSELs. A schematic diagram of the current oxidation system is shown in Fig. 1. The nitrogen inlet gas (derived from liquid N_2 boil off) is dried and purified before entering the mass flow controller. The gas is then passed through a 2 ft. coil of stainless tubing submerged in the constant temperature bubbler bath to preheat the gas prior to entering the water bubbler. The 5 liter Pyrex bubbler flask is submerged in a 26 liter constant temperature bath of silicon oil. The bath temperature regulation is specified at ± 0.005 °C. There is also a K-type thermocouple submerged in the water (not touching the flask) to monitor the actual

MASTER

DISTRIBUTION OF THIS DOCUMENT IS UNLIMITED

DISCLAIMER

This report was prepared as an account of work sponsored by an agency of the United States Government. Neither the United States Government nor any agency thereof, nor any of their employees, make any warranty, express or implied, or assumes any legal liability or responsibility for the accuracy, completeness, or usefulness of any information, apparatus, product, or process disclosed, or represents that its use would not infringe privately owned rights. Reference herein to any specific commercial product, process, or service by trade name, trademark, manufacturer, or otherwise does not necessarily constitute or imply its endorsement, recommendation, or favoring by the United States Government or any agency thereof. The views and opinions of authors expressed herein do not necessarily state or reflect those of the United States Government or any agency thereof.

DISCLAIMER

Portions of this document may be illegible in electronic image products. Images are produced from the best available original document.

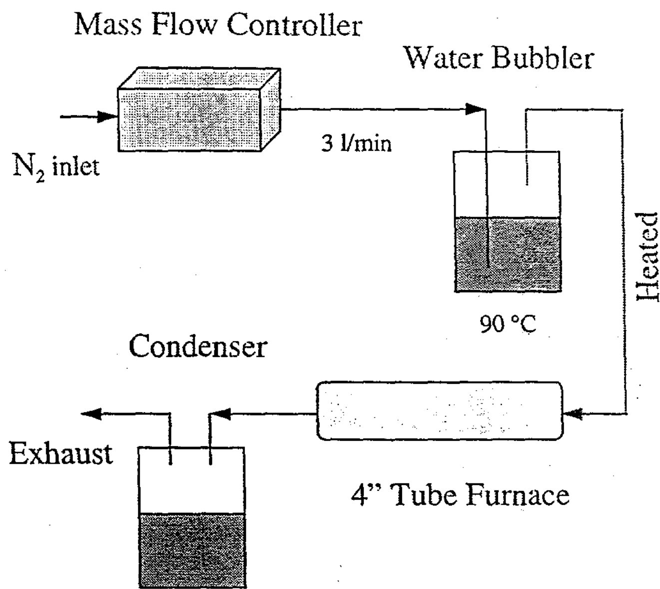

Figure 1. A schematic diagram of the compound semiconductor oxidation system.

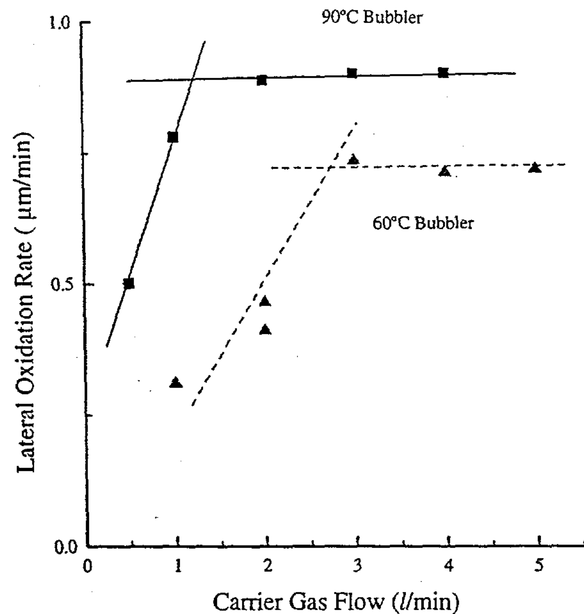

Figure 2. Buried layer oxidation rates in steam at 440°C for different bath temperatures and carrier gas flow rates.

water temperature. The 1/2" OD Teflon plumbing between the bubbler and the furnace is maintained at a temperature of 150 °C using heating tape to prevent condensation of water vapor from the gas stream. The furnace is a 3 foot long 3 zone Lindberg tube furnace with digital temperature controllers which provide a temperature regulation of ±1.0°C. The exhaust gas from the furnace is extracted from a port on the side of the quartz furnace tube into the laboratory exhaust system providing a safe exhaust for any toxic gases that might be evolved. The condenser between the furnace and the exhaust prevents excessive water condensation in the laboratory exhaust system.

The amount of water vapor that can be transferred into the N_2 gas stream is proportional to the water temperature in the bubbler. This effect is manifest as a change in oxidation rate with a change in the bath temperature as shown in Fig. 2. Notice that both curves saturate at about 2.5 *l*/min. gas flow but at different oxidation rates due to the difference in H_2O vapor concentration level. To achieve maximum water vapor into the gas stream, the bath is kept just below the boiling point at 90 °C (boiling point at Albuquerque's 5500 ft elevation is ~94.5 °C). Even with the constant temperature bath, there is a measurable variation in the water temperature with gas flow. Figure 3 shows the water temperature measured using the thermocouple immersed in the bubbler as a function of N_2 flow. The bath temperature remains constant for a given flow indicating that there is enough insulation between the bath oil and the water to support this equilibrium temperature differential. The strong gas flow dependence seen in Fig.'s 2 and 3 indicates the need for good repeatability in the carrier gas flow which is provided by the mass flow controller.

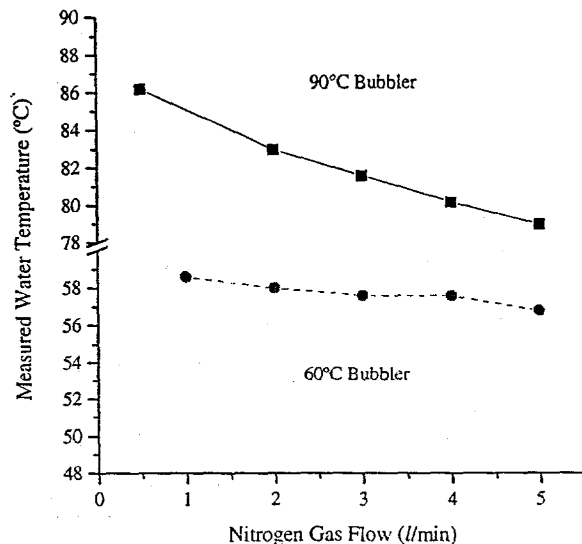

Figure 3. Equilibrium water temperature as a function of flow rate for two different constant temperature bath settings.

Furnace temperature calibration was accomplished using three K-type thermocouples: one thermocouple located in the center of the furnace with the other two offset at opposite ends of the boat giving a test zone of 6 inches. The thermocouples were placed in intimate contact with the boat since the oxidation samples, which lie parallel to the gas flow on the flat boat, will be in thermal equilibrium with the boat. Note that the boat temperature is somewhat different than the gas temperature due to the heat sink of the furnace walls and that all of the temperatures described in the following sections correspond to the boat temperature rather than the gas temperature. Careful adjustment of the set point temperatures of the 3 furnace zones results in a 'flat zone' along the 6" boat with less than one degree variation at a 3 *l*/min. carrier gas flow as shown in Fig. 4a. The measured boat temperatures are also a strong function of the moisture content in the inlet gas as shown in Fig. 4b and c reemphasizing the need for stable bubbler temperature control. This degree of temperature and gas flow calibration and control should be considered as the minimum required to insure repeatable oxidation for VCSEL fabrication.

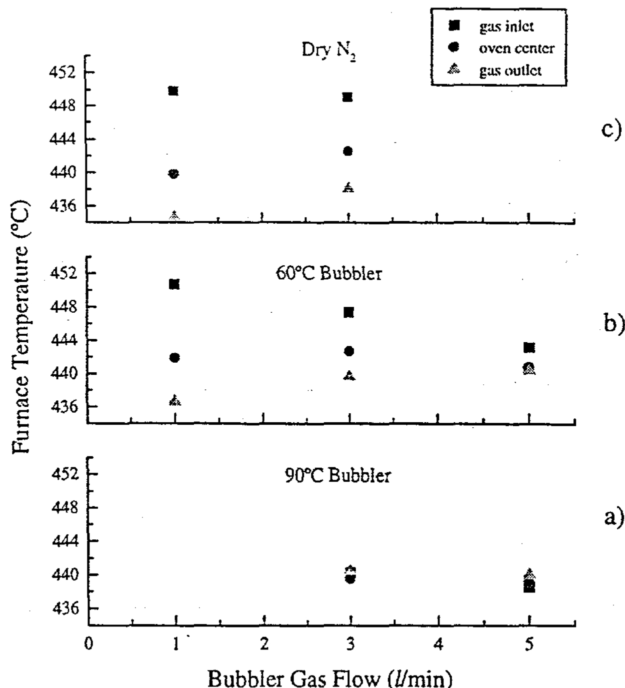

Figure 4. Furnace boat surface temperatures measured at 3 positions as a function of moisture content in the gas flow: a) highest H_2O vapor content, b) lower H_2O vapor content, c) no H_2O vapor (dry N_2).

3. OXIDATION RATES

The oxidation rate data was obtained in the system described above using 850 nm VCSEL structures grown with a single 1/4 wavelength thick high Al content layer (98%) near the active region in the top distributed Bragg reflector (DBR)[2,11]. The samples were grown using an EMCORE GS3200 metalorganic vapor phase epitaxy rotating disc reactor which provides extremely good (± 0.2%) compositional uniformity across the 3" wafer as is required for accurate oxidation rate experiments[12]. The alloy composition was parabolically graded across the heterointerfaces of high and low Al containing layers to reduce series electrical resistance in the laser mirrors. The oxidation rates for $Al_xGa_{1-x}As$ compositions of x=0.98 and 0.92 were measured from the same wafer, while the AlAs rates were obtained from a second wafer. All of the oxidation rate measurements were made from 110μm square mesas on 125μm centers to maintain a similarity to the VCSEL mesas used for device fabrication. The oxidation extent was determined by measuring the amount of unoxidized material left after oxidation in an infared microscope and subtracting that value from the mask mesa size. This technique was used due to the difficulty in accurately observing both the mesa edge and the unoxidized region simultaneously. The lateral extent of oxidation was averaged over the 2 orthogonal mesa directions to remove any systematic sample orientation effects in the furnace. The mesas were dry etched in a reactive ion etching system which typically produced nearly vertical sidewalls. Systematic error in the measurement results in a linear offset that is about the same for all of the samples and is estimated to be ±1 μm. The boat was pulled from the hot furnace, samples were placed on the hot boat and moved back into the system within 10 seconds. The oxidation time is defined as when the sample boat reaches the center of the furnace until when the boat is pulled out of the furnace.

A typical monolithic oxide-confined VCSEL structure produced at Sandia National Laboratories uses an AlAs mole fraction of 92% in the low index distributed Bragg reflector layers and 98% for the buried oxide aperture[2,9]. We also include the AlAs oxidation rate for completeness but its use for oxide-confined VCSELs is not recommended due to oxide stress issues[13]. Typical oxidation extents for our VCSELs are between 10 and 50 microns and we employ total oxidation times that are relatively short but easy to control: 10-20 min. Within these constraints, the lateral oxidation rate is linear for all of the temperatures, times, and compositions investigated as shown in Fig. 5a. Note that there is sufficient selectivity in the oxidation rate to allow the buried 98% layer to oxidize about 3 times faster than the 92% layers. The linear fits to the data in Fig. 5 do not all pass through the origin due to the small variation between the mask and the actual mesa size as mentioned above. Figure 5b shows the temperature dependence of the oxidation rate of 98% AlGaAs for a wide range of temperatures. The data shows the repeatability of the experiment and the linearity of the rate at the various temperatures. Our oxidation

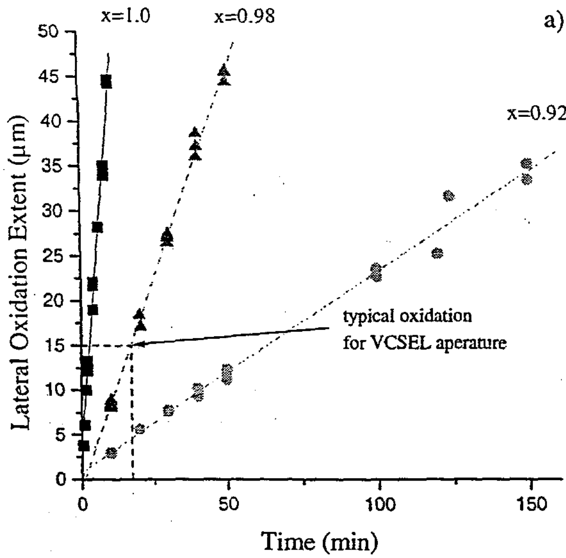

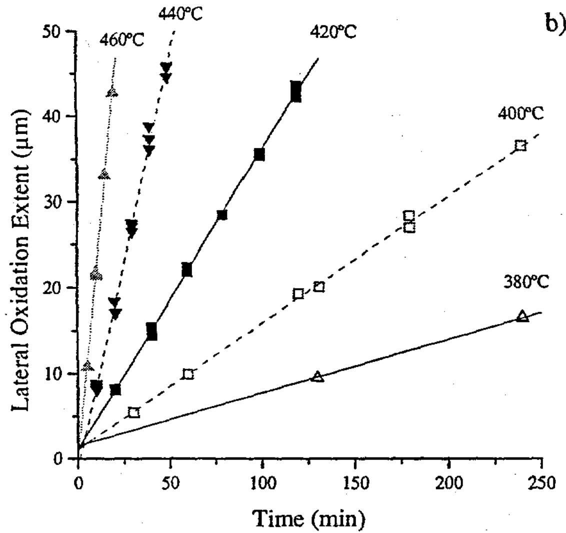

Figure 5. Lateral oxidation extents in steam for a) Al$_x$Ga$_{1-x}$As at 440°C (x=1.00, 0.98, 0.92), b) Al$_{0.98}$Ga$_{0.2}$As at 5 different temperatures. The arrow indicates our standard VCSEL oxidation condition.

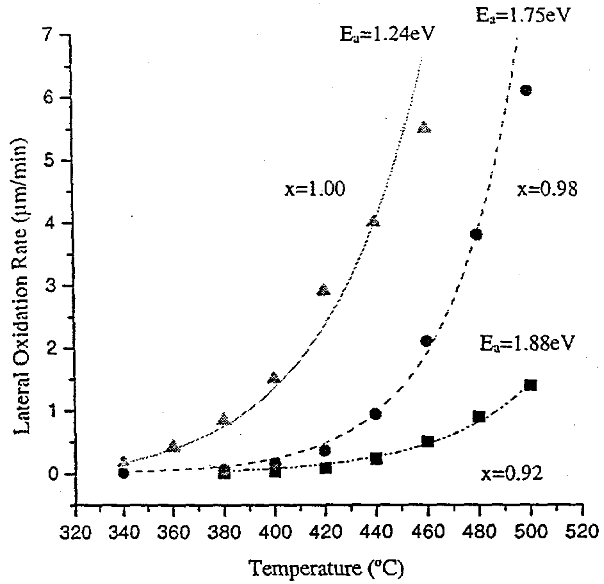

Figure 6. Saturated steam oxidation rate data showing an exponential fit and the extracted Arrhenius activation energies for three AlAs mole fractions.

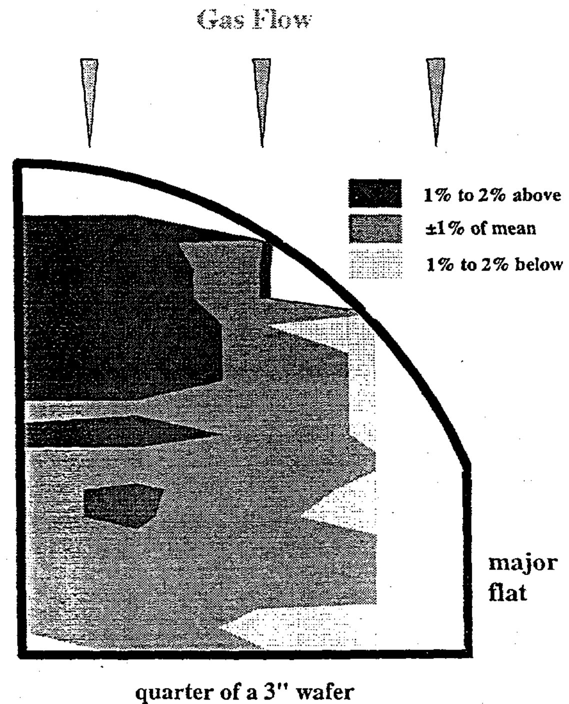

Figure 7. Contour plot of measured oxidation rates across a quarter of a 3" VCSEL wafer oxidized in steam at 440°C with the sample placed parallel to the gas flow as indicated by the arrows.

Table 1. AlGaAs oxidation rates in microns per minute for 3 different compositions.

temperature	92%	98%	100%
340 °C		0.00914	0.160
360 °C			0.412
380 °C	0.0121	0.0622	0.839
400 °C	0.0301	0.147	1.48
420 °C	0.0815	0.346	2.91
440 °C	0.226	0.937	4.02
460 °C	0.497	2.14	5.46
480 °C	0.899	3.77	
500 °C	1.40	6.09	

operating condition for VCSEL fabrication is indicated in Fig. 5a, where we typically operate at 440°C for ~18 min. to oxidize ~15 μm.

A compilation of the rates measured over a 1 year time span are given in Table 1 and plotted in Fig. 6. The temperature dependence can be fit to an exponential curve due to its Arrhenius relationship. The oxidation rate activation energies from the various Al compositions are shown in Fig. 6; for comparison the wet thermal oxidation energy of Si is 1.96 eV[14]. The variation in activation energy for the various Al compositions is indicative of the significant oxidation rate selectivity between 98% and 92% AlGaAs which is exploited for VCSEL fabrication[2].

We also see excellent oxidation uniformity across one quarter of a 3" wafer as seen in Fig. 7. The oxidation rate is slightly lower on the down stream side of the wafer presumably due to H_2O vapor depletion. However, the variation in rate is less than ± 2% across the entire surface. Assuming this oxidation rate variation is due only to wafer compositonal nonuniformity and using an exponential fit to the rate versus composition curve, yields a compositional range of x=0.9795 to 0.9810 for the nominally 98% AlGaAs. Thus we conclude that our oxidation process is sufficiently uniform, even in the presence of AlAs mole fraction variations of 1×10^{-3}.

4. CONCLUSIONS

Strict control of the AlAs mole fraction, the water (bath) temperature, sample temperature, and gas flow rate are all important for repeatable and uniform oxide-confined VCSEL fabrication. We have presented data showing that a carefully designed oxidation system can give reproducible oxidation rates that are appropriate for the manufacture of high performance selectively oxidized VCSEL arrays. We find that the resulting oxidation rates are linear with time over a large temperature range for Al mole fractions of 92% to 100% and that there is sufficient selectivity to Al composition for fabricating monolithic VCSELs with buried oxide apertures. As VCSELs emerge into the marketplace in present and new applications, high performance devices based on fabrication processes such as described here will likely be utilized.

5. ACKNOWLEDGMENTS

Sandia is a multiprogram laboratory operated by Sandia Corporation, a Lockheed Martin Company, for the United States Department of Energy under Contract DE-AC04-94AL85000.

8. REFERENCES

1. J. M. Dallesasse, N. Holonyak, Jr., A. R. Sugg, T. A. Richard, and N. El-Zein, "Hydrolyzation oxidation of Al_xGa_{1-x}-AlAs-GaAs quantum well heterostructures and superlattices," *Appl. Phys. Lett.* **57** (26), pp. 2844-2846, 1990.
2. K. D. Choquette, R. P. Schneider, Jr., K. L. Lear, and K. M. Geib, "Low threshold voltage vertical-cavity lasers fabricated by selective oxidation," *Electron. Lett.* **30** (24), pp. 2043-2044, 1994.
3. D. L. Huffaker, D. G. Deppe, K. Kumar, and T. J. Rogers, "Native-oxide defined ring contact for low threshold vertical-cavity lasers," *Appl. Phys. Lett.* **65** (1), pp. 97-99, 1994.
4. G. M. Yang, M. H. Macdougal, and P. D. Dapkus, "Ultralow threshold current vertical-cavity surface-emitting lasers obtained with selective oxidation," *Electron. Lett.* **31** (11), pp. 886-888, 1995.
5. K. L. Lear, K. D. Choquette, R. P. Schneider, Jr., S. P. Kilcoyne, and K. M. Geib, "Selectively oxidized vertical-cavity surface emitting lasers with 50% power conversion efficiency," *Electron. Lett.* **31** (3), pp. 208-209, 1995.
6. B. Weigl, G. Reiner, M. Grabherr, and K. J. Ebeling, "Oxidised GaAs QW vertical-cavity lasers with 40% power conversion efficiency," *Electron. Lett.* **32** (19), pp. 1784-1786, 1996.
7. K. L. Lear, S. P. Kilcoyne, R. P. Schneider, Jr., and J. A. Nevers, "Life-testing oxide confined VCSELs: too good to last?," *Fabrication, Testing, and Reliability of Semiconductor Lasers*, ed. M. Fallahi and S. C. Wang, vol. **2683**, pp. 114-122 (SPIE, San Jose, 1996).
8. R. S. Burton, and T. E. Schlesinger, "Use of a native oxide of $Al_xGa_{1-x}As$ in the fabrication of integrated laser/modulators," *Mat. Res. Soc. Symp. Proc.* **300**, pp. 127-132, 1993.
9. K. D. Choquette, K. L. Lear, R. P. Schneider, Jr., K. M. Geib, J. J. Figiel, and R. Hull, "Fabrication and performance of selectively oxidized vertical-cavity lasers," *IEEE Photon. Technol. Lett.* **7** (11), pp. 1237-1239, 1995.

10. M. Ochiai, G. E. Giudice, H. Temkin, J. W. Scott, and T. M. Cockerill, "Kinetics of thermal oxidation of AlAs in water vapor," *Appl. Phys. Lett.* **68** (14), pp. 1898-1900, 1996.
11. K. D. Choquette, K. M. Geib, H. C. Chui, H. Q. Hou, and R. Hull, "Selective oxidation of buried AlGaAs for fabrication of vertical-cavity lasers," *Mat. Res. Soc. Symp. Proc.* **421**, pp. 53-61, 1996.
12. H. Q. Hou, H. C. Chui, K. D. Choquette, B. E. Hammons, and W. G. Breiland, "Highly uniform and reproducible vertical-cavity surface-emitting lasers grown by metalorganic vapor phase epitaxy with in situ reflectometry," *IEEE Photon. Technol. Lett.* **8** (10), pp. 1285-1287, 1996.
13. K. D. Choquette, K. M. Geib, H. C. Chui, B. E. Hammons, H. Q. Hou, T. J. Drummond, and R. Hull, "Selective oxidation of buried AlGaAs versus AlAs layers," *Appl. Phys. Lett.* **69** (10), pp. 1385-1387, 1996.
14. L. E. Katz, "Oxidation," in *VLSI technology*, ed. S.M. Sze, pp. 137-139 (McGraw-Hill Book Company, New York, 1983).